Mem. S.A.It. Vol. 7, 12
© SAIt 2005

Memorie della
Supplementi

Radio spectroscopy of active galactic nuclei

A. P. Lobanov

Max-Planck-Institut für Radioastronomie, Auf dem Hügel 69, 53121 Bonn, Germany
e-mail: alobanov@mpifr-bonn.mpg.de

Abstract. Radio spectroscopy offers a number of tools for studying a large variety of astrophysical phenomena, ranging from stars and their environment to interstellar and intergalactic medium, active galactic nuclei (AGN) and distant quasars. Main targets of extragalactic radio spectroscopy are atomic and molecular material in galaxies, H II regions, and maser emission originating in the dense, circumnuclear regions. These studies cover all galactic types and span an impressive range of angular scales and distances. Molecular emission, hydrogen absorption and maser lines have become the tools of choice for making an assessment of physical conditions in the nuclear regions of galaxies. In this contribution, some of the recent advances in the aforementioned fields will be reviewed and discussed in connection with future radio astronomical facilities.

Key words. Radio lines: galaxies – Galaxies: active – Galaxies: nuclei

1. Introduction

Spectroscopic observations in the radio domain present remarkable opportunities to study chemical composition and kinematics of plasma, gas, and molecular material in stars, galaxies and galactic nuclei (Verschuur & Kellermann 1988). This makes radio spectroscopy an excellent counterpart to spectral studies made in other bands. Radio spectroscopy spans an impressive spectral range of frequencies (0.1 GHz to 500 GHz, Fig. 1), reaches out to redshifts in excess of 5 (Klamer et al. 2005), and operates at angular scales down to a fraction of milliarcsecond, using the techniques of connected and long baseline interferometry. Radio spectroscopic studies of active galaxies (AG) and active galactic nuclei (AGN) embrace both broad-band and narrow band spectral measurements, probing non-thermal emission from cosmic plasmas as well as thermal and maser radiation from various atomic and molecular species. Observations of water masers in AGN have paved the way to detailed studies of inner accretion disks and accurate measurements of black hole masses (Moran et al. 1995). Measurements of synchrotron self-absorption have been used to determine the physical conditions in AGN on sub-parsec scales (Lobanov 1998a). Hydrogen and free-free absorption toward bright continuum sources has become a powerful tool to probe the circumnuclear environment in galaxies (Conway 1999; Walker et al. 2000). Physical conditions in relativistic outflows from AGN can be probed effectively by studying the distribution and evolution of the turnover frequency of the synchrotron emission from parsec-scale jets (Lobanov 1998b). Observations of molecular lines, the CO lines in particular, have become

Send offprint requests to: A. P. Lobanov

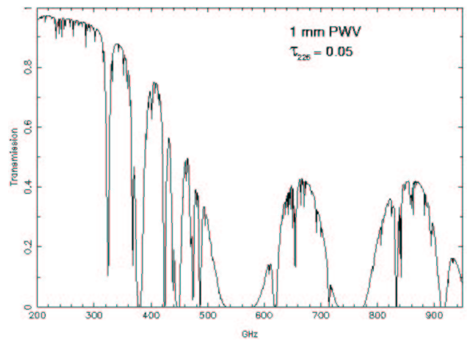

Fig. 1. Atmospheric transmission for frequencies up to 1000 GHz. Below 500 GHz (λ = 0.6 mm), absorption due to water in the Earth atmosphere does not play a significant role and a large number of atomic and molecular lines can be observed using ground based facilities working in centimeter and millimeter bands. Above 500 GHz and outside the two main windows at 350 μm and 450 μm, observations can only be made with airborne and space observatories. (Courtesy of the Steward Observatory Radio Astronomy Laboratory.)

a tool of choice to probe the galactic activity up to very high redshifts (Klamer et al. 2005). Radio recombination lines (Kardashev 1959) have been detected so far only in a small number of extragalactic objects (Gordon & Sorochenko 2002) and can be used as an effective indicator of the physical state of ionized material in galaxies. The next generation of radio astronomical instruments: LOFAR (at 10–240 MHz), SKA (300 MHz–43 GHz), and ALMA (30–1000 GHz) will be most actively involved in radio spectroscopy, achieving up to two orders of magnitude increase in sensitivity and opening new horizons for spectroscopic studies in the radio domain.

2. Atomic lines

With the exception of recombination lines, atomic radio lines are rare, as most atomic transitions produce spectral lines at wavelengths in the infrared or shorter. Table 1 lists the atomic radio lines, including the famous 21 cm (1.42 GHz) hyperfine line of neutral hydrogen. The D I line at 327 MHz is the deuterium analogue of the 21 cm line of H I. The D I line has not yet bet detected, even inside our Galaxy (Heiles et al. 1993), probably because most of the deuterium in the Universe is in the molecule HD (Tielens 1983). The radio lines of both H I and D I are cosmologically important, as they can be used to measure directly the primordial composition of matter in the Universe. The hyperfine spin-flip transition of $^3He^+$ has been detected in a number of Galactic sources (Bania et al. 1997). The C I lines are used as tracers of molecular gas in the central regions of galaxies (Israel & Baas 2002) and at high redshifts (Weiss et al. 2003; Papadopoulos et al. 2004).

Table 1. Parameters of atomic radio lines

Line	Transition	ν/GHz	Det.
D I	$^2S_{1/2}, F = 3/2 - 1/2$	0.327	no
H I	$^2S_{1/2}, F = 1 - 0$	1.420	G,E
$^3He^+$	$^2S_{1/2}, F = 0 - 1$	8.665	G
C I	$^3P_1 - ^3P_0$	492.16	G,E
C I	$^3P_2 - ^3P_1$	809.34	G

Note: The last column shows whether a given line has been detected in Galactic (G) and extragalactic (E) objects.

2.1. Hydrogen line

The 21 cm line of H I is a "work horse" of spectroscopy in the radio domain. It has been used most successfully to study the characteristics of diffuse interstellar medium in the Milky Way and in other galaxies. The H I line is characterized by its spin temperature T_s (the excitation temperature for hyperfine transitions). Several processes contribute to T_s, including (i) absorption and emission stimulated by external photon radiation field; (ii) collisions with hydrogen atoms and free electrons; (iii) "pumping" by Ly α photons Field (1959). This allows estimates of various properties of H I emitting material to be made (Rohlfs & Wilson 2004). In addition, the Zeeman effect of a frequency shift of the circularly polarized components of H I line profile (both in emission and in absorption) enables direct measurements of the line-of-sight magnitude of the magnetic field.

Observations of neutral hydrogen in galaxies is a prime tool for studying the distribution and motion of interstellar gas in galaxies. For a galaxy at a distance d, the mass of neutral hydrogen can be estimated from

$$M_{\rm HI}[M_\odot] = 2.36\times10^5\, d^2 \int S_\nu {\rm d}\,v\,,$$

where S_ν is in Jy and the line is integrated over velocity in km s^{-1}. Observations of H I line have been used to study galactic rotation and determine the mass distribution in a number of spiral galaxies (Bosma 1981). These have provided the basis for the virial mass estimates for the central regions of galaxies and for the famous Tully-Fisher (1976) relation connecting the maximum rotational velocity and luminosity of galaxies. Mapping the H I distribution in relatively close galaxies shows that (i) the H I is not centrally concentrated and its extent is larger than the optical extent; (ii) the rotation appears to be flattening at large distances (in contrast to the decrease observed in the optical rotation curve); (iii) H I links and bridges exist between galaxies separated by a few tens of kiloparsecs. At present, the brightness sensitivity of existing instruments sets an angular resolution limit of ∼ 5 arcsec for studies of H I emission and precludes detailed measurements close to active nuclei. The situation should change with the SKA providing a factor of 100 improvement of sensitivity. It should also be noted that, besides galactic studies, observations of H I have a paramount importance for cosmological investigations, most notably for studies of structure formation and the epoch of re-ionization.

2.2. Recombination lines

Recombination lines are produced by electrons bound to ions and cascading downwards in the energy levels. Observability of recombination lines in the radio regime was predicted by Kardashev (1959). There is a large number of radio recombination lines (RRL) in the 1–500 GHz range. Wavelengths of recombination lines of an atom with a total mass M are given by the well-known Rydberg formula

$$\lambda(n,\Delta n) \simeq \frac{1}{R_{\rm M}\,Z^2}\left[\frac{1}{n^2} - \frac{1}{(n+\Delta n)^2}\right]^{-1}\,,$$

where $R_{\rm M}$ is the atomic Rydberg constant, Z is the effective charge of the nucleus, n is the lower principal quantum number, and $\Delta n \ll n$ is the change in n. Thus, for α-transitions, with $\Delta n = 1$, the wavelengths of recombination lines exceed 1 cm for $n > 60$ (see Fig 2).

RRL can be used to estimate temperatures (from the ratio of line energy to that of the underlying free-free continuum), densities (from the line broadening), and kinematics (from the Doppler modification of the line shape and center frequency). RRL have been observed throughout our own Galaxy (Gordon & Sorochenko 2002), most notably in the Galactic H II regions (Georgelin & Georgelin 1976; Odegard 1985). The first extragalactic detection of a recombination line was made

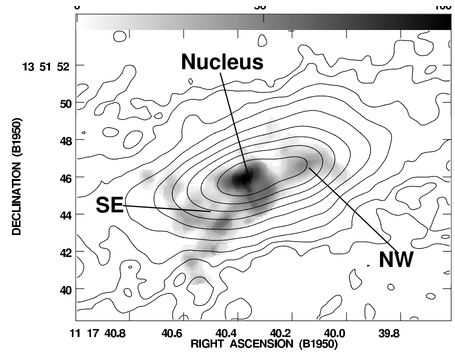

Fig. 2. Integrated H92α line flux image of the nuclear region of NGC 3628. The line is produced by the α-transition from the energy level with $n = 92$ ($\lambda = 3.608$ cm,). The gray-scale range is 0–100 mJy beam^{-1} km s^{-1}. The contours represent the continuum flux densities of 0.04, 0.08, 0.16, 0.32, . . . , 10.3 mJy beam^{-1}. Labeled are three RRL emission components: Nucleus, SE, and NW. The position-velocity distribution of the RRL emission implies a rotating circumstellar disk with a total dynamical mass of 3×10^8 M$_\odot$ within a distance of 120 pc from the nucleus (Zhao et al. 1997).

almost 30 years ago in M 82 (Shaver et al. 1977), but the total number of RRL detections in other galaxies is small, and no detections of RRL in quasars have been reported so far. Observations of RRL over a wide range of quantum levels provides valuable information on the physical state of the ionized gas (Anantharamaiah et al. 1993). High-resolution observations of RRL (Fig. 2) can be used to determine velocity fields in galactic nuclei at an arcsecond resolution, and dynamics of the galaxies and especially the nuclear regions can be studied (Zhao et al. 1997).

3. Molecular lines

Molecular line emission is produced via three different types of energy transitions: (i) electronic transitions, with typical energies of ∼ 5 eV (gives lines in the visual and UV spectrum); (ii) vibrational transitions (from oscillations of the relative positions of nuclei with respect to their equilibrium positions), with typical energies of 0.01–0.1 eV corresponding to lines in the infrared band; (iii) rotational transitions, with typical energies of $\simeq 10^{-3}$ eV corresponding to lines in the millimeter and centimeter ranges.

Molecular line radio astronomy began in 1963, with a detection of absorption by the OH molecules of continuum radio emission from supernova remnant Cassiopeia A. Contrary to the atomic, radio lines from molecules provide a vastly richer field of study, with a total of over 120 molecular species identified in the circumstellar medium and more than 20 molecular species detected toward extragalactic regions (Mauersberger & Henkel 1993; Mauersberger et al. 2003). Molecular gas has been detected in more than 650 galaxies (Verter 1990), and the number of detections is increasing every year. Among the most common molecules detected in other galaxies (Table 2) are hydroxyl (OH), methanol (CH_3OH), formaldehyde (H_2CO), ammonia NH_3, hydrogen cyanide (HCN), formylium (HCO^+), silicon monoxide (SiO), and carbon monoxide (CO). Ammonia (NH_3) is a good temperature indicator of extragalactic molecular gas. The CO and HCN emission and absorption are good tracers of the mass of the molecular gas in galaxies, and they can nowadays be detected over an enormous range of column density at millimeter wavelengths (Liszt & Lucas 1998). Observations of CO toward powerful AGN imply that the molecular gas is highly structured in the nuclear regions (Fig. 3). However, here again, the sensitivity of modern instruments does not permit direct studies of molecular emission at a resolution needed to probe directly the conditions in circumnuclear regions in galaxies.

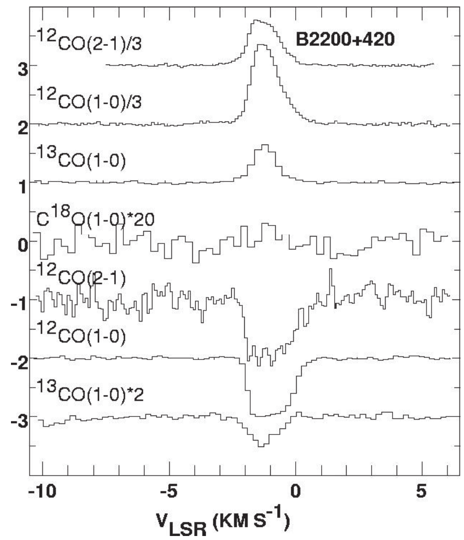

Fig. 3. CO absorption and emission profiles toward BL Lac. The spectra indicate a surprisingly one-dimensional structure of the molecular gas, as a fully-formed line profile is observed from an integration along the line of sight to a point source of ∼ 1 mas in size. This implies that the material producing the molecular emission is highly structured (Liszt & Lucas 1998).

4. Maser lines

The first detection of an astronomical maser was made thirty years ago (Weaver et al. 1965), with a definitive answer about the maser nature of the object coming from very long baseline (VLBI) observations (Moran et al. 1968).

Table 2. Commonly observed molecular lines

Line	Transition	ν/GHz
OH	$^2\Pi_{3/2}F = 1 - 2$	1.61223
OH†	$^2\Pi_{3/2}F = 1 - 1$	1.66540
OH†	$^2\Pi_{3/2}F = 2 - 2$	1.66736
OH	$^2\Pi_{3/2}F = 2 - 1$	1.720529
$CH_3OH^\dagger$	$J_K = 5_1 - 6_0A^+$	6.66852
$CH_3OH^\dagger$	$J_K = 2_0 - 3_1E$	12.17859
H_2CO	$J_{K_\alpha K_c} = 2_{11} - 2_{12}$	14.48849
$H_2O^\ddagger$	$J_{K_\alpha K_c} = 6_{16} - 5_{23}$	22.23525
NH_3	$(J, K) = (1, 1) - (1, 1)$	23.69451
NH_3	$(J, K) = (2, 2) - (2, 2)$	23.72263
SiO†	$J = 1 - 0, v = 2$	42.82059
SiO†	$J = 1 - 0, v = 1$	43.12208
SiO	$J = 1 - 0, v = 0$	43.42386
SiO†	$J = 2 - 1, v = 2$	85.64046
SiO†	$J = 2 - 1, v = 1$	86.24344
SiO	$J = 2 - 1, v = 0$	86.84700
HCN†	$J = 1 - 0, F = 2 - 1$	88.63185
HCO^+	$J = 1 - 0$	89.18852
$C^{18}O$	$J = 1 - 0$	109.78218
^{13}CO	$J = 1 - 0$	110.20137
CO	$J = 1 - 0$	115.27120

Notes: † – often found in maser transitions; ‡ – always found in maser transitions (from Rohlfs & Wilson 2004)

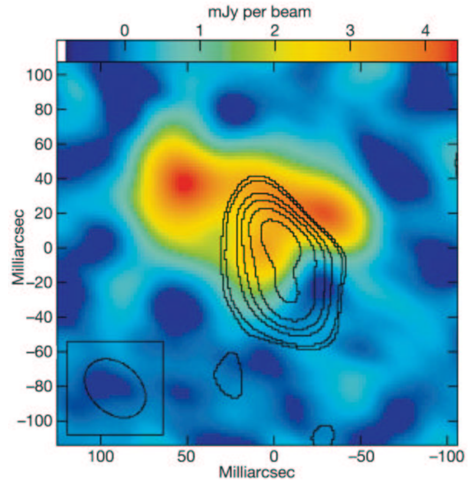

Fig. 4. The integrated OH (pseudo-color) and radio-continuum (contours) emission in the nucleus of Mrk 231. The hydroxyl (mega)-maser emission shows the characteristics of a rotating, dusty, molecular torus (or thick disk) located within 30–100 pc from the central engine (Klöckner et al. 2003).

Subsequently, a number of Galactic and extragalactic masers have been discovered and studied. Five major types of cosmic masers are known to date (Table 2): (i) H_2O masers at 22.2 GHz (1.3 cm); (ii) OH masers at 1.67 GHz (18 cm); (iii) methanol (CH_3OH) masers at 6.67 GHz (5 cm); (iv) silicon monoxide (SiO) masers at 43.1 GHz (0.7 cm) and 86.2 GHz (0.3 cm); (v) HCN masers at 88.6 GHz (0.3 cm) — and many other molecules exhibit weaker maser emission. All Galactic masers are produced in the circumstellar envelopes and near young stars.

4.1. OH megamasers

Extragalactic maser emission was first discovered in NGC 253 in the 1665 MHz and 1667 MHz transitions of OH (Whiteoak & Gardner 1974) with a luminosity of about 100 times greater than typical Galactic OH masers. In 1982 an OH "megamaser" was discovered in Arp220 (IC 4553) (Baan et al. 1982). Since then, more than 50 extragalactic OH sources have been discovered (Baan 1993). The OH megamasers are characterized by much higher luminosities and broader emission lines (up to several 100 km s^{-1}) compared to Galactic OH masers. The standard model of the OH megamasers assumes a low-gain amplification in a molecular disk around the nucleus of the galaxy (Norris 1984). The gas is pumped by far-infrared radiation (Baan 1989) and amplifies the nuclear continuum emission. Extragalactic OH megamasers often found in ultra-luminous FIR galaxies (ULIRG), which are generally characterized by morphological peculiarities, interactions with neighbors, highly ionized species showing starburst and AGN-type nuclear phenomena (Klöckner & Baan 2005). The OH megamasers are reported to have a two-component structure (Fig. 4), with a compact and diffuse maser emission, possibly tracing an interaction between the ionization cones of the outflow and the molecular torus (Klöckner et al. 2003).

4.2. H_2O megamasers

In 1977, a small number of H_2O masers have been detected in several nearby spiral galaxies (Churchwell et al. 1977), all of them similar to the Galactic masers. Extragalactic "megamasers", with luminosities in excess of $100\,L_\odot$, were discovered in nuclei of active galaxies (dos Santos & Lepine 1979; Claussen & Lo 1986), and soon after became an impressive tool to study the circumnuclear regions in AGN (with more than 20 megamasers known to date; Maloney 2002). Most of the H_2O megamasers have been detected in Seyfert 2 and LINER galaxies, but the situation has changed with the detection of a maser in the radio-loud galaxy 3C 403 (Tarchi et al. 2003).

All known H_2O megamasers have the following common properties: (i) host galaxies show evidence for nuclear activity (Braatz et al. 1996; 1997); (ii) the maser emission is centered on the nucleus; (iii) the spatial diameter of the emitting regions is small (< 3 pc) (Greenhill et al. 1995; Miyoshi et al. 1995).

Extragalactic H_2O masers are used in a variety of studies including (i) mapping accretion disks in AGN, (ii) determining the mass of the central black holes, (iii) obtaining geometric distances to galaxies (Fig. 5; Herrnstein et al. 1998), (iv) studying the interaction between the dense molecular material and the ionization cones (Gallimore et al. 1996; Greenhill et al. 2001) and nuclear jets (Claussen et al. 1998; Peck et al. 2003), and (v) measuring proper motions of maser spots in the local group of galaxies (Brunthaler et al. 2005).

5. Absorption lines

In the radio domain, absorption due to several atomic and molecular species has been detected, most notably due to H I, CO, OH, and HCO^+ (see Table 2). In many cases, absorbing material lies in our own galaxy (Liszt & Lucas 2000). In extragalactic objects, OH absorption has been used to probe the conditions in warm neutral gas (Goikoechea et al. 2004; Klöckner & Baan 2005). Observations of CO and H I absorption have been used to study the molecular tori (Conway 1999; Pedlar 2004) at

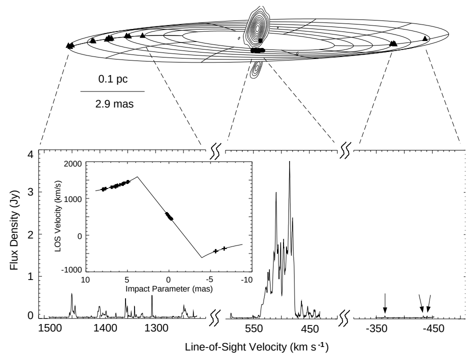

Fig. 5. H_2O masers in NGC 4258. Top panel: actual maser positions (filled triangles and circles) superimposed on the radio-continuum emission (contours) and approximated by a model of warped disk. The filled square marks the best-fit location of the center of the disk. Bottom panel: total spectrum of the maser emission and line-of-sight velocities of individual spots fitted by a Keplerian disk model. The high-velocity masers trace a Keplerian curve to better than 1%. Observations of H_2O masers in NGC 4258 have allowed to infer a geometric distance of 7.2 ± 0.3 Mpc to the galaxy from the direct measurement of orbital motions in the maser spots. The motions imply a central object with a mass of $(3.9 \pm 0.1) \times 10^7\,M_\odot$ (Herrnstein et al. 1998).

a linear resolution often smaller than a parsec (Mundell et al. 2003). These observations have revealed, in particular, the morphology and kinematics of neutral gas in the molecular torus in NGC 4151 (Fig. 6) and in a rotating outflow surrounding the relativistic jet in 1946+708 (Peck & Taylor 2001).

6. Broad-band spectrum

Broad-band emission from AGN is dominated by non-thermal synchrotron and inverse-Compton radiation from highly accelerated plasma. The synchrotron mechanism plays a more prominent role in the radio domain, and the properties of the emitting material can be assessed using the turnover point in the synchrotron spectrum (Lobanov 1998b), syn-

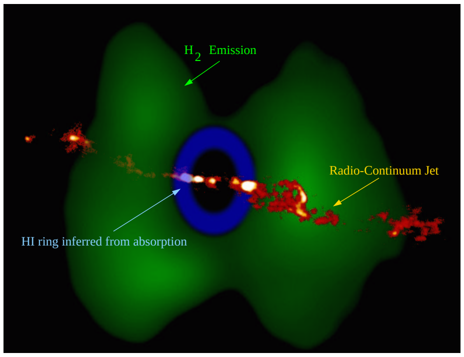

Fig. 6. Montage of the inner 250 pc of NGC 4151. The H_2 emission traces a torus, the H I absorption comes from a ring inside the torus. Ionized gas (black) is assumed to fill the torus inside the H I ring (Mundell et al. 2003).

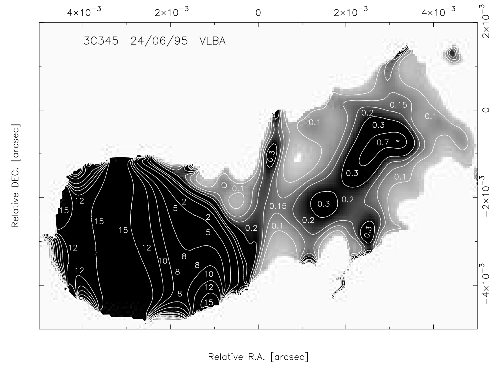

Fig. 7. Distribution of the turnover frequency in the jet of 3C 345 obtained from fitting multifrequency VLBI data. Values of the turnover frequency (in GHz) are shown next to the corresponding contours. Values below 1 GHz are upper limits. The distribution implies the presence of strong shocks within ~ 1 mas (~ 5 pc) of the nucleus. At larger distances, the shocks dissipate and give way to Kelvin-Helmholtz instabilities indicated by oblique patterns of higher turnover frequency (Lobanov 1998b).

chrotron self-absorption (Lobanov 1998a), and free-free absorption in the plasma (Walker et al. 2000; Kadler et al. 2004). The free-free absorption studies indicate the presence of dense, ionized circumnuclear material with $T_e \approx 10^4$ K distributed within a fraction of parsec from the central nucleus (Lobanov 1998a; Walker et al. 2000). Mapping the turnover frequency distribution (Fig. 7) provides a sensitive diagnostics of shocks and plasma instabilities in the relativistic flows (Lobanov et al. 1997; Lobanov 1998b).

7. Conclusions

Radio spectroscopy offers a variety of tools that can be used to assess and quantify the physical conditions in galaxies and active galactic nuclei. Observations of neutral hydrogen, recombination and molecular lines provide a wealth of information about the gas dynamics on galactic scales. However, the limited sensitivity of present-day instruments does not allow to use the line emission to study structures on sub-arcsecond scales.

Maser lines and absorption lines can be studied at highest resolution, even with the existing instruments. Maser emission, although detected in a modest number of extragalactic objects, provides an impressive opportunity to detect and monitor processes in accretion disks on scales of less than a parsec. Absorption towards compact extragalactic jets presents an effective tool to diagnose the properties of circumnuclear gas associated with the molecular tori and sub-relativistic outflows in AGN.

The field of radio spectroscopy will be revolutionized with the next-generation radio astronomy facilities planned to be built in the near future. A brightness temperature sensitivity as low as 100-10000 K at angular scales as small as a few milliarcseconds will become feasible in the millimeter and centimeter domains. Quasar molecular absorption lines will be observed in the spectra of many sources. The optically-obscured molecular tori and the circumnuclear starbursts of nearby galaxies will be resolved. The presence of central black holes will be studied kinematically in a large number of galaxies. This will open a truly new era in the studies of active galactic nuclei.

Acknowledgements. I would like to express my sincere gratitude to the conference organizers for their great support and warm hospitality during the meeting.

References

Anantharamaiah, K. R., et al. 1993, ApJ, 419, 585.
Baan, W. A. 1989, ApJ, 338, 804
Baan, W. A. 1993, in Davis R. J., Booth R. S., eds, Subarcsecond Radio Astronomy. Cambridge Univ. Press, Cambridge, p. 324
Baan, W. A., Wood, P. A. D., & Haschick, A. D. 1982, ApJ, 260, L49
Bania, T. M., et al. 1997, ApJS, 113, 353
Bosma, A. 1981, AJ, 86, 1825
Braatz, J. A., Wilson, A. S., & Henkel, C. 1996, ApJS, 106, 51
Braatz, J. A., Wilson, A. S., & Henkel, C. 1997, ApJS, 110, 321
Brunthaler, A., et al. 2005, Science, 307, 1440
Churchwell, E. A., et al. 1977, A&A, 54, 969
Claussen, M. J., & Lo, K. Y. 1986, ApJ, 308, 592
Claussen, M. J., et al. 1998, ApJ, 500, L129
Conway, J. E. 2005, NewAR, 43, 509
DiMatteo, T., et al. 2002, ApJ, 564, 576
dos Santos, P. M., & Lepine, J. R. D. 1979, Nature, 278, 34
Field, G. B. 1959, ApJ, 129, 536
Gallimore, J. F., et al. 1996, ApJ, 462, 740
Georgelin, Y. M., & Georgelin, Y. P. 1976, A&A, 49, 57
Goikoechea, J. R., Martin-Pintado, J., & Chernicharo, J. 2004, ApJ, 619, 291
Gordon, M. A., & Sorochenko, R. L. 2002, Radio Recombination Lines, Their Physics and Astronomical Applications, (Kluwer: Dordrecht)
Greenhill, L. J., et al. 1995, ApJ, 304, 21.
Greenhill, L. J., et al. 2001, in Proceedings of IAU Symposium 205, ed. R. T. Schilizzi, 334
Heiles, C., McCullough, P. R., & Glassgold, A. E. 1993, ApJS, 89, 271
Herrnstein, J. R., et al. 1998, Nature, 400, 539
Herrnstein, J. R., et al. 2005, ApJ *(in press)* (astro-ph/0504405)
Israel, F. P., & Baas, F. 2002, å, 323, 82
Klöckner, H. R., & Baan, W. A. 2005, Astrophysics and Space Science, 295, 277
Klöckner, H. R., Baan, W. A., & Garrett, M. A. 2003, Nature, 421, 821
Kadler, M., et al. 2004, A&A, 426, 481
Kardashev, N. S. 1959, Sov. Astron., 3, 813
Klamer, I. J., Ekers, R. D., Sadler, E. M., et al. 2005, AJ, 621, L1
Liszt, H. S., & Lucas, R. 1998, A&A, 339, 561
Liszt, H. S., & Lucas, R. 1998, A&A, 355, 333
Lobanov, A. P. 1998a, A&A, 379, 90
Lobanov, A. P. 1998b, A&ASS, 120, 30.
Lobanov, A. P., Carrara, E., & Zensus, J. A. 1997, Vistas in Astronomy, 41, 253
Maloney, P. R. 2002, PASA, 19, 401
Mauersberger, R., & Henkel, C. 1993, Rev. Mod. Astronomy, 6, 69
Mauersberger, R., et al. 2003, A&A, 403, 561
Miyoshi, M. et al. 1995, Nature, 373, 127
Moran, J. M., et al. 1968, ApJ, 152, L97
Moran, J., Greenhill, L., Herrnstein, J., et al. 1995, PNAS, 92, 25, 11427
Mundell, C. G., et al. 1999, MNRAS 304, 481.
Mundell, C. G., et al. 2003, ApJ, 583, 192
Norris, R. P. 1984, PASA, 5, 514
Odegard, N. 1985, ApJS, 57, 571
Papadopoulos, P. P., Thi, W.-F., & Viti, S. 2004, MNRAS, 351, 147
Peck, A. B., & Taylor, G. B. 2001, ApJ, 554, 147
Peck, A. B., et al. 2003, ApJ, 590, 149
Pedlar, A. 2004, Ap&SS, 295, 161
Rohlfs, K., & Wilson, T. L. 2004, Tools of Radio Astronomy, (Springer: Heidelberg)
Shaver, P. A., Churchwell, E., & Rots, A. H. 1977, A&A, 55, 435
Tarchi, A., et al. 2003, A&A, 407, L33
Tielens, A. G. G. M. 1983, A&A, 119, 117
Tully, R. B., & Fisher, J. R. 1976, A&A, 54, 661
Verschuur, G. L., & Kellermann, K. I. (eds.) 1988, Galactic and Extragalactic Radio Astronomy, (Springer-Verlag: Heidelberg)
Verter, F. 1990, PASP, 102, 1281
Walker, R. C., et al. 2000, ApJ, 530, 233
Weaver, H., et al. 1965, Nature, 208, 29
Weiss, A., et al. 2003, A&A, 409, L41
Whiteoak, J. B., & Gardner, F. F. 1974, ApJ, 15, L211
Zhao, J.-H., et al. 1997, ApJ, 482, 186